

Nuclear magnetic shielding of noble gases in liquid crystals

Mika Ylihautala, Juhani Lounila, and Jukka Jokisaari

Citation: *The Journal of Chemical Physics* **110**, 6381 (1999); doi: 10.1063/1.478541

View online: <http://dx.doi.org/10.1063/1.478541>

View Table of Contents: <http://scitation.aip.org/content/aip/journal/jcp/110/13?ver=pdfcov>

Published by the AIP Publishing

Articles you may be interested in

Measuring the spin polarization of alkali-metal atoms using nuclear magnetic resonance frequency shifts of noble gases

AIP Advances **5**, 107119 (2015); 10.1063/1.4932131

Nuclear magnetic shielding constants of liquid water: Insights from hybrid quantum mechanics/molecular mechanics models

J. Chem. Phys. **126**, 034510 (2007); 10.1063/1.2424713

Comment on "Calculation of nuclear magnetic shieldings using an analytically differentiated relativistic shielding formula" [J. Chem. Phys. **123**, 114102 (2005)]

J. Chem. Phys. **124**, 137101 (2006); 10.1063/1.2181968

Relativistic effects on the nuclear magnetic shieldings of rare-gas atoms and halogen in hydrogen halides within relativistic polarization propagator theory

J. Chem. Phys. **123**, 214108 (2005); 10.1063/1.2133729

Relativistic, nearly basis-set-limit nuclear magnetic shielding constants of the rare gases He–Rn: A way to absolute nuclear magnetic resonance shielding scales

J. Chem. Phys. **118**, 2973 (2003); 10.1063/1.1545718



NEW Special Topic Sections

NOW ONLINE
Lithium Niobate Properties and Applications:
Reviews of Emerging Trends

AIP Applied Physics Reviews

Nuclear magnetic shielding of noble gases in liquid crystals

Mika Ylihautala,^{a)} Juhani Lounila, and Jukka Jokisaari

NMR Research Group, Department of Physical Sciences, University of Oulu, P.O. Box 3000, FIN-90401 Oulu, Finland

(Received 28 September 1998; accepted 30 December 1998)

A theoretical model for nuclear magnetic shielding of noble gas atoms soluted in liquid crystal solvents is developed. It is found that the solvent effect on the shielding can be represented as a linear combination of products of the liquid crystal orientational order parameters of varying rank. In a special case of pairwise additive shielding perturbations, most of the coefficients vanish and the shielding reduces to a sum of two terms, the isotropic and anisotropic parts. Both contributions are directly proportional to the density of the liquid crystal, and the anisotropic part is also directly proportional to the second rank orientational order parameter of the liquid crystal. The developed model is used to account for the behavior of the ^{129}Xe shielding in the nematic liquid crystal 4-ethoxybenzylidene-2,6-dideutero-4'-n-butylaniline (d_2 -EBBA). The pairwise additivity approximation of the shielding perturbations is found to explain the observed temperature dependence of the ^{129}Xe shielding satisfactorily. In particular, the temperature dependence of the isotropic part is mostly due to the change in the liquid crystal density, whereas the anisotropic part is mainly controlled by the temperature dependence of the Xe-liquid crystal molecule pair correlation function and the second rank orientational order parameter of the liquid crystal. This result differs from the results of the phenomenological theory of Lounila *et al.* [J. Chem. Phys. **97**, 8977 (1992)], where only the density and the orientational order parameter were assumed to be significantly temperature dependent. © 1999 American Institute of Physics. [S0021-9606(99)50913-6]

I. INTRODUCTION

NMR spectroscopy of noble gas atoms in different environments has many applications in materials research. Liquids, liquid crystals, polymers, and zeolites are commonly investigated, especially with the aid of ^{129}Xe NMR.^{1,2} Moreover, the increased sensitivity achieved with the new laser polarization technique has widened the area of ^{129}Xe and ^3He NMR to surface phenomena investigations and imaging applications.³ One reason for the popularity of noble gas NMR is the sensitivity of noble gas nuclear magnetic shielding (σ) to its environment. Particularly, ^{129}Xe has a wide chemical shift range (~ 300 ppm) in different environments, allowing to probe detailed properties of various systems.

For the applications of noble gas NMR, the understanding of different factors affecting the shielding is essential. For an isolated noble gas atom in an external magnetic field, the shielding induced by the electron cloud can be calculated quantum mechanically, and it is found to be diamagnetic.⁴ However, in solution such calculation is not feasible, because the system consists of a noble gas atom surrounded by a cluster of solvent molecules, all subject to motion. Consequently, a more phenomenological approach is usually applied to describe the solvent induced change of the solute shielding (σ_m). The solvent can modify the solute shielding in two ways: by changing the local magnetic field experi-

enced by the solute, and by distorting the electronic cloud of the solute. The former includes bulk susceptibility effect (σ_b), and the effect of the magnetic anisotropy of the neighboring solvent molecules (σ_a). The latter can be divided into the effects due to the long range attractive van der Waals (σ_w) and short range repulsive (σ_{rep}) interactions.

Apart from macroscopic σ_b , the solvent effects on the solute shielding are microscopic and depend on the local surrounding of solute. In the present work, we develop a statistical mechanical approach to the evaluation of σ_m in the case of a noble gas atom dissolved into a nematic liquid crystal. In general, it is found that the solute shielding can be written as a linear combination of products of liquid crystal orientational order parameters of varying rank. However, such a model is not practical for analysis purposes, due to the large number of coefficients in the expression. Consequently, we utilize the assumption of *pairwise additivity* of the solvent induced change of the shielding in order to simplify the expression. Such an assumption was recently used to develop group contributonal analysis method to explain the differences in ^{129}Xe shieldings between several isotropic liquids.⁵ The result in a nematic solvent reduces to a simple form, which is the sum of the isotropic and anisotropic parts. Both contributions are directly proportional to the density of the liquid crystal, and the anisotropic contribution is also proportional to the second rank orientational order parameter of the liquid crystal. Finally, the validity of the pairwise additivity theory of shielding is tested in case of xenon dissolved in the

^{a)} Author to whom correspondence should be addressed. Electronic mail: mika.ylihautala@oulu.fi

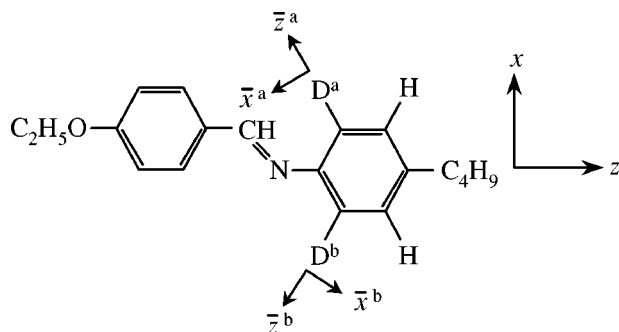


FIG. 1. The molecular structure of deuterated EBBA. The principal axis system of the electric field gradient tensor for deuterons *a* and *b* are indicated by $(\bar{x}^a, \bar{y}^a, \bar{z}^a)$ and $(\bar{x}^b, \bar{y}^b, \bar{z}^b)$, respectively. Coordinate system (x, y, z) is used for the presentation of the average electric field gradient tensor.

nematic liquid crystal 4-ethoxybenzylidene-2,6-dideutero-4'-n-butylaniline (*d*₂-EBBA).

II. EXPERIMENT

Partially deuterated form of the liquid crystal EBBA (4-ethoxybenzylidene-2,6-dideutero-4'-n-butylaniline, Fig. 1) was used to allow the determination of orientational order of the liquid crystal from ²H NMR spectrum. *d*₂-EBBA was placed in a heavy wall sample tube (diameter, 10 mm; wall thickness, 1 mm), and was carefully degassed prior to natural abundance xenon gas transfer (2 atm) and flame sealing.

²H and ¹²⁹Xe single pulse NMR spectra were measured on a JEOL GX-400 spectrometer without lock. Single scan was sufficient in order to get reasonable signal-to-noise ratio for ¹²⁹Xe spectra (resonance frequency, 110.61 MHz), whereas accumulation of 16 scans was needed for ²H spectra (61.38 MHz). The chemical shift of ¹²⁹Xe was referenced to the corresponding low-pressure pure gas signal.

III. THEORY

The microscopic part of solvent induced nuclear magnetic shielding of a solute is affected only by the nearest neighboring molecules, that is, solute shielding is a property of a microscopic cluster of molecules. The shielding tensor of the solute, $\bar{\sigma}(\mathbf{x}, \mathbf{x}^n)$, depends on the positions and orientations of the solute and surrounding solvent molecules, denoted by \mathbf{x} and \mathbf{x}^n , respectively. Here \mathbf{x}^n is the short-hand notation for $\mathbf{x}_1, \mathbf{x}_2, \dots, \mathbf{x}_n$, where \mathbf{x}_i is used to indicate both the positional (\mathbf{r}_i) and orientational (Ω_i) coordinates of the *i*th solvent molecule with respect to a laboratory fixed coordinate system, and \mathbf{x} represents the corresponding coordinates of the solute (see Fig. 2). The thermal fluctuations of the positions and orientations modify the shielding tensor. However, these fluctuations are very fast on the NMR time scale and consequently an average shielding tensor is observed. In dilute solution such an average can be expressed as^{6,7}

$$\langle \bar{\sigma} \rangle = \int d\mathbf{x} d\mathbf{x}_1 \cdots d\mathbf{x}_n p^{(n+1)}(\mathbf{x}, \mathbf{x}^n) \bar{\sigma}(\mathbf{x}, \mathbf{x}^n). \quad (1)$$

Here the $(n+1)$ -particle distribution function $p^{(n+1)}(\mathbf{x}, \mathbf{x}^n)$ is the probability for the existence of the configuration $(\mathbf{x}, \mathbf{x}^n)$

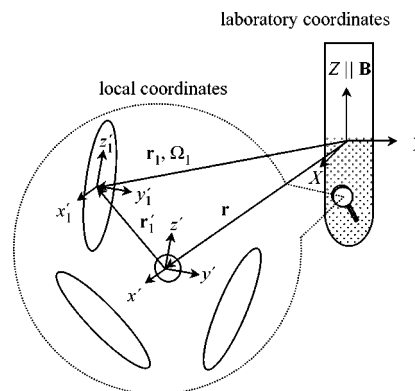


FIG. 2. The definitions of the laboratory (X, Y, Z) and local (x', y', z') coordinate systems. The origin of the local coordinate system is located at the position of the solute, and its orientation with respect to the laboratory coordinate system is determined by the orientation of the solvent molecule 1.

and is determined by its energy according to the Boltzmann statistics. It is advantageous to rewrite $p^{(n+1)}(\mathbf{x}, \mathbf{x}^n)$ as the product of the solute and solvent single particle distribution functions $p_0(\mathbf{x})$ and $p(\mathbf{x}_i)$, respectively, and the $(n+1)$ -particle correlation function $g^{(n+1)}(\mathbf{x}, \mathbf{x}^n)$ (Refs. 6, 7)

$$p^{(n+1)}(\mathbf{x}, \mathbf{x}^n) = p_0(\mathbf{x}) p(\mathbf{x}_1) \cdots p(\mathbf{x}_n) g^{(n+1)}(\mathbf{x}, \mathbf{x}^n). \quad (2)$$

The more easily accessible information is included in the single particle distribution functions, whereas the complicated part is included in the correlation function $g^{(n+1)}(\mathbf{x}, \mathbf{x}^n)$.

The momentary value of the shielding tensor of the solute depends on the *relative* positions and orientations of the solvent molecules with respect to the solute, rather than on the actual position of solute. Because the shielding is a tensor property, its value depends also on the choice of the coordinate system. If the coordinate system is fixed to the instantaneous configuration of the solvent molecules, an invariable shielding tensor of the solute with respect to a rotation of the specific configuration is achieved (see Fig. 2). We term it as a *local* coordinate system. The *laboratory* frame value of the shielding tensor, however, changes in rotation. Its value can be obtained by a coordinate transformation from the local frame:

$$\sigma_{lk} = \sum_{m=-l}^l D_{mk}^l(\Omega') \sigma'_{lm}. \quad (3)$$

Here the irreducible spherical tensor representation of the shielding tensor elements is used, and the local frame values are distinguished from the laboratory frame values by prime. $D_{mk}^l(\Omega')$ is the Wigner rotation matrix, whose argument Ω' (i.e., the three Euler angles) defines the orientation of the local coordinate system with respect to the laboratory one.

The momentary configuration $(\mathbf{x}, \mathbf{x}^n)$, defined with the help of the laboratory coordinates, can be alternatively specified by utilizing the local coordinate system. In that case, the local coordinates are used to specify the relative positions and orientations of the solute and solvent with respect to each other. This is termed as a local configuration. Then the laboratory coordinates are used to determine the momentary

orientation and position of the local configuration. The natural choice for the origin of the local coordinate system is the solute, whose position is indicated by \mathbf{r} . However, there is no equally natural choice for the orientation of the local coordinate system in the case of spherical solutes like atoms. In that case, the orientation of the local coordinate system can be chosen as the orientation of one of the neighboring molecules, for example $\Omega' \equiv \Omega_1$ (see Fig. 2). Consequently, Ω_1 and \mathbf{r} specify the momentary orientation and position of the local configuration with respect to the laboratory frame, whereas $(\mathbf{r}'_1, \mathbf{x}'_2, \dots, \mathbf{x}'_n)$ determine the momentary local configuration (prime indicates local coordinate representation, and for the first solvent molecule only the position \mathbf{r}'_1 with respect to the solute atom is required, see Fig. 2). Now the solute shielding in the local coordinates can be written as $\sigma'_{lm}(\mathbf{x}, \mathbf{x}') \equiv \sigma'_{lm}(\mathbf{r}'_1, \mathbf{x}'_2, \dots, \mathbf{x}'_n)$.

In case of a noble gas dissolved in a nematic liquid crystal (LC), one deals with a homogenous system. Consequently, the single particle distribution function of the solute is the constant

$$p_0(\mathbf{x}) = \frac{1}{8\pi^2 V}, \quad (4)$$

where V is the volume of the sample. In a nematic phase, the LC solvent molecules may possess orientational order, although no positional order exists. Because any well behaved

function of the three Euler angles can be expanded in a series of Wigner rotation matrices, the single particle distribution function of the solvent molecule can be written as

$$p(\mathbf{x}_i) = \frac{1}{V} \sum_{lmn} a'_{lmn} D^l_{mn}(\Omega_i). \quad (5)$$

Here the Euler angles Ω_i specify the LC molecule orientation with respect to laboratory frame and the coefficients $a'_{lmn} = (2l+1)/(8\pi^2) \langle D^l_{mn}(\Omega_i)^* \rangle_{\Omega_i}$ are directly proportional to the orientational order parameters of LC. The summation indices l , m , and n fulfill the usual requirements for the Wigner matrices. The above single particle distribution function of an LC molecule is determined in the laboratory coordinates. However, in order to exploit the local configuration representation introduced above, we need the probability for the orientation Ω'_i of the i th LC molecule with respect to the local coordinate system, which is further oriented at Ω_1 with respect to the laboratory frame. That can be obtained from Eq. (5) by applying the closure property of the Wigner matrices:

$$p(\mathbf{x}'_i) (= p(\mathbf{x}_i)) = \frac{1}{V} \sum_{lmnk} a^l_{mn} D^l_{mk}(\Omega_1) D^l_{kn}(\Omega'_i). \quad (6)$$

Substitution of Eqs. (2)–(6) in Eq. (1) gives

$$\begin{aligned} \langle \sigma_{lk} \rangle = & \frac{1}{V^n} \sum_{l_1 m_1 n_1} \sum_{l_2 m_2 n_2} \cdots \sum_{l_n m_n n_n} \sum_m a^{l_1}_{m_1 n_1} \cdots a^{l_n}_{m_n n_n} \\ & \times \underbrace{\int_{\Omega_1} D^{l_1}_{m_1 n_1}(\Omega_1) D^{l_2}_{m_2 n_2}(\Omega_1) \cdots D^{l_n}_{m_n n_n}(\Omega_1) D^l_{mk}(\Omega_1) d\Omega_1}_{\text{orientational average}} \\ & \times \underbrace{\int_{\mathbf{r}'_1} \int_{\mathbf{x}'_2} \cdots \int_{\mathbf{x}'_n} \sigma'_{lm}(\mathbf{r}'_1, \mathbf{x}'_2, \dots, \mathbf{x}'_n) g^{(n+1)}(\mathbf{r}'_1, \mathbf{x}'_2, \dots, \mathbf{x}'_n) D^{l_2}_{k_2 n_2}(\Omega'_2) \cdots D^{l_n}_{k_n n_n}(\Omega'_n) d\mathbf{r}'_1 d\mathbf{x}'_2 \cdots d\mathbf{x}'_n}_{\text{configurational average}}, \end{aligned} \quad (7)$$

where we have assumed that the correlation function $g^{(n+1)}$ also depends only on the relative coordinates of the solute and solvent, that is, $g^{(n+1)}(\mathbf{x}, \mathbf{x}') \equiv g^{(n+1)}(\mathbf{r}'_1, \mathbf{x}'_2, \dots, \mathbf{x}'_n)$. It indicates that the effect of the LC molecules outside the microscopic cluster of molecules, and the effect of the external fields on the correlation function are negligible as compared to the intermolecular interactions of the solute and the n solvent molecules. The above sum contains two different averages, the first one representing the orientational behavior of the local frame with respect to the laboratory frame, i.e., the orientational behavior of the local cluster. The second one represents the average elements of the local shielding tensor over the different local configurations.

In an NMR experiment, the average of the shielding tensor element in the direction of the external magnetic field (Z) is observed. In spherical tensor notation, that is

$$\langle \sigma_{zz} \rangle = \sqrt{\frac{2}{3}} \langle \sigma_{20} \rangle - \frac{1}{\sqrt{3}} \langle \sigma_{00} \rangle. \quad (8)$$

The number of the terms in the sum of Eq. (7) can be considerably reduced, if the symmetry properties of the mesophase are taken into account. In case of cylindrically symmetric solvent molecules constituting the nematic phase, the only nonvanishing coefficients $a^{l_i}_{m_i n_i}$ are those for which l_i is even and $m_i = n_i = 0$. A straightforward substitution of the

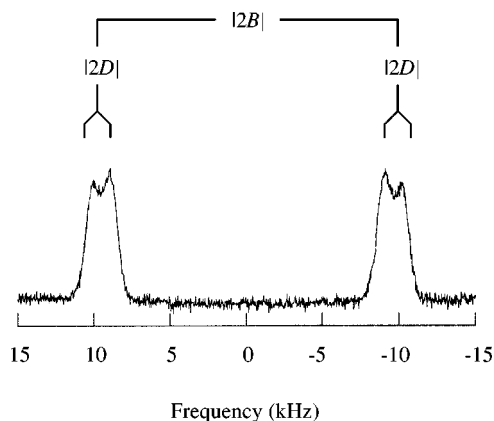


FIG. 3. ^2H NMR spectrum of deuterated EBBA. The only resolved couplings are the quadrupolar and dipolar coupling to the nearest proton indicated by B and D , respectively. The magnitude of the dipolar couplings to the other protons as well as the spin-spin couplings are vanishing and can be seen only as “broadenings” of the resonances.

above results shows that in a nematic phase the average shielding of a noble gas atom induced by the LC molecules is a linear combination

$$\langle \sigma_{ZZ} \rangle = \sum_{l_1, \dots, l_n} \xi(l_1, \dots, l_n) \bar{P}_{l_1} \bar{P}_{l_2} \dots \bar{P}_{l_n}. \quad (9)$$

Here $\bar{P}_{l_i} = 8\pi^2/(2l_i+1)a_{00}^{l_i} \langle P_{l_i}(\cos \theta) \rangle$ is the LC molecule orientational order parameter of rank l_i with respect to the external magnetic field (θ is the angle between the external magnetic field and the long axis of the LC molecule). Coefficients ξ are proportional to different combinations of the configurational and orientational averages [see Eq. (7)]. The result shows rather surprising dependence of $\langle \sigma_{ZZ} \rangle$ also on the higher than the second rank orientational order parameters of the liquid crystal molecules.

The application of Eq. (9) is hampered by the large number of terms in the sum. In order to simplify it we adopt the assumption of pairwise additivity of the solute shielding perturbation. In other words, the total solute shielding is obtained by summing over all the shielding perturbations induced by the individual solute-solvent pairs, that is, $\bar{\sigma}(\mathbf{x}, \mathbf{x}^N) = \sum_{i=1}^N \bar{\sigma}(\mathbf{x}, \mathbf{x}_i)$. Here we have summed over all the solvent molecules of the sample (N), which is of course more accurate than summing only over the n nearest solvent molecules. For an individual solute atom-solvent molecule pair the average shielding reduces to

$$\begin{aligned} \langle \sigma_{ZZ} \rangle_{\text{pair}} &= \sqrt{\frac{2}{3}} \frac{1}{V} \bar{P}_2 \int_{\mathbf{r}_1'} \sigma'_{20}(\mathbf{r}_1') g^{(2)}(\mathbf{r}_1') d\mathbf{r}_1' \\ &\quad - \frac{1}{\sqrt{3}} \frac{1}{V} \int_{\mathbf{r}_1'} \sigma'_{00}(\mathbf{r}_1') g^{(2)}(\mathbf{r}_1') d\mathbf{r}_1' \\ &= \frac{1}{V} \left(\langle \sigma \rangle_{\mathbf{r}_1'} + \frac{2}{3} \langle \Delta \sigma \rangle_{\mathbf{r}_1'} \bar{P}_2 \right), \end{aligned} \quad (10)$$

where the orthogonality of the Wigner matrices has been used. Moreover, in the latter form the notations $\Delta \sigma$

$= \sqrt{3/2} \sigma'_{20}$ for the anisotropy and $\sigma = -\sigma'_{00}/\sqrt{3}$ for the isotropic part of the shielding tensor have been adopted. If the actual solute-solvent pair correlation function in solution is used, the total shielding is obtained simply by multiplying Eq. (10) with the number of solvent molecules:

$$\langle \sigma_{ZZ} \rangle = \rho (\langle \sigma \rangle_{\mathbf{r}_1'} + \frac{2}{3} \langle \Delta \sigma \rangle_{\mathbf{r}_1'} \bar{P}_2). \quad (11)$$

Here $\rho = N/V$ is the solvent number density. Note that this is the same result as obtained in the phenomenological theory of Lounila *et al.*⁸ in the nematic phase (where the translational and translational-orientational order parameters τ_1 and σ_1 are zero) Eq. (8) of Ref. 8 is equivalent to Eq. (11). Consequently, it proves that the basic assumptions used in Ref. 8, i.e., that the perturbation on the shielding is directly proportional to the density ρ and the anisotropy of the perturbation is directly proportional to the orientational order parameter \bar{P}_2 , are correct, provided that the shielding perturbations are pairwise additive.

The average solute shielding is temperature dependent via the temperature dependence of the distribution functions. The temperature dependence of the single particle distribution functions is directly seen in the solute shielding as a change of liquid crystal density and orientational order parameters [see Eq. (7)]. However, the change of the correlation function is seen only indirectly via the change of the configurational averages of the local shielding tensor elements. In the case of pairwise additive shielding the indirect temperature dependence is included in $\langle \sigma \rangle_{\mathbf{r}_1'}$ and $\langle \Delta \sigma \rangle_{\mathbf{r}_1'}$. In isotropic phase of LC, where the orientational order is missing, the shielding of noble gas solute is known to change linearly with temperature at least within a moderate temperature range. Moreover, the relative change is very close to the relative change of the solvent density.⁸ Therefore, it is reasonable to assume that changes in the pair correlation function are small, and consequently $\langle \sigma \rangle_{\mathbf{r}_1'}$ and $\langle \Delta \sigma \rangle_{\mathbf{r}_1'}$ are slowly varying functions of temperature. In fact, in the phenomenological theory of Lounila *et al.*⁸ only the density ρ and the orientational order parameter \bar{P}_2 were assumed to be significantly temperature dependent, and the parameters corresponding to $\langle \sigma \rangle_{\mathbf{r}_1'}$ and $\langle \Delta \sigma \rangle_{\mathbf{r}_1'}$ were taken to be constants. However, in the present theory the temperature dependence of $\langle \sigma \rangle_{\mathbf{r}_1'}$ and $\langle \Delta \sigma \rangle_{\mathbf{r}_1'}$ is allowed for, by approximating them in the neighborhood of a point T_0 by the linear functions

$$\langle \sigma(T) \rangle_{\mathbf{r}_1'} = \langle \sigma(T_0) \rangle_{\mathbf{r}_1'} + \left(\frac{\partial \langle \sigma \rangle_{\mathbf{r}_1'}}{\partial T} \right)_{T_0} (T - T_0), \quad (12)$$

$$\langle \Delta \sigma(T) \rangle_{\mathbf{r}_1'} = \langle \Delta \sigma(T_0) \rangle_{\mathbf{r}_1'} + \left(\frac{\partial \langle \Delta \sigma \rangle_{\mathbf{r}_1'}}{\partial T} \right)_{T_0} (T - T_0). \quad (13)$$

Then the temperature dependent pairwise additive shielding can be written as

$$\langle \sigma_{zz} \rangle = \rho(T) \left\{ \sigma_0 [1 - \epsilon(T - T_0)] + \frac{2}{3} \Delta \sigma_0 [1 - \Delta \epsilon(T - T_0)] \bar{P}_2(T) \right\}, \quad (14)$$

where the notations $\sigma_0 = \langle \sigma(T_0) \rangle_{r'_1}$, $\epsilon = -(1/\langle \sigma(T_0) \rangle_{r'_1}) \times (\partial \langle \sigma \rangle_{r'_1} / \partial T)_{T_0}$, $\Delta \sigma_0 = \langle \Delta \sigma(T_0) \rangle_{r'_1}$, and $\Delta \epsilon = (-1/\langle \Delta \sigma(T_0) \rangle_{r'_1}) (\partial \langle \Delta \sigma \rangle_{r'_1} / \partial T)_{T_0}$ have been used.

IV. RESULTS AND DISCUSSION

A. Orientational order parameter of EBBA

In order to get information on the anisotropy of the liquid crystal environment, the ^2H NMR spectrum of d_2 -EBBA

was measured as a function of temperature. The spectrum consists of four resolved signals, from which the quadrupolar coupling and dipolar coupling to the nearest proton can be identified (see Fig. 3). The similar values of the quadrupolar and dipolar couplings for both deuterons most likely indicate that the fast intramolecular motions make the deuterons equivalent. We assume that such a result is a consequence of a two site jump model, in which the aniline ring undergoes fast 180° rotations around the z -axis (see Fig. 1). Consequently, the electric field gradient (EFG) tensors of the deuterons average to the same value $(\bar{V}^a + \bar{V}^b)/2$, where \bar{V}^i is the EFG tensor at the position i ($i=a,b$, see Fig. 1).⁹ In the molecule fixed (x,y,z) -coordinates defined in Fig. 1, the average EFG tensor is

$$\bar{V} = \begin{pmatrix} \frac{1}{4}(V'_{xx} + 3V'_{zz}) & 0 & \frac{\sqrt{3}}{8}(V'_{xx} - V'_{yy} + V'_{zz} - V'_{zz}) \\ 0 & V'_{yy} & 0 \\ \frac{\sqrt{3}}{8}(V'_{xx} - V'_{yy} + V'_{zz} - V'_{zz}) & 0 & \frac{1}{4}(3V'_{xx} + V'_{zz}) \end{pmatrix}, \quad (15)$$

where we have assumed hexagonal geometry for the aniline ring. Notation $V'_{ii} = (V_{ii}^a + V_{ii}^b)/2$ ($i=x,y,z$, see Fig. 1) is adopted for the average of the EFG tensor principal values at the positions a and b . If the principal values at these positions do not differ significantly from each other, the above nondiagonal values vanish, and the averages are

$$V'_{xx} \approx \frac{1}{2}eq'(\eta' - 1), \quad V'_{yy} \approx -\frac{1}{2}eq'(\eta' + 1), \quad (16)$$

$$V'_{zz} = eq',$$

where $q' = (q^a + q^b)/2$ and $\eta' = (\eta^a + \eta^b)/2$ [$eq^i = V_{zz}^i$ is the EFG value along the CD^i -bond and $\eta^i = (V_{xx}^i - V_{yy}^i)/V_{zz}^i$ is the asymmetry parameter for the deuteron i ($i=a,b$)].

In addition to the internal motion, the quadrupolar coupling is modified by the reorientational motions of the d_2 -EBBA molecule. Consequently, the observed quadrupolar coupling is

$$B = \frac{eQ}{2h} \left\{ S_{zz} \left[V_{zz} - \frac{1}{2}(V_{xx} + V_{yy}) \right] + \frac{1}{2}(S_{xx} - S_{yy})(V_{xx} - V_{yy}) \right\} \\ = \frac{e^2Qq'}{32h} [S_{zz}(9\eta' - 3) + (S_{xx} - S_{yy})(5\eta' + 9)], \quad (17)$$

where eQ is the nuclear quadrupole moment, h is the Planck constant, and S_{ii} is the orientational order parameter of the i -axis ($i=x,y,z$) with respect to the external magnetic field. Note that the Cartesian Saupe ordering tensors have been

adopted here instead of the spherical tensor representation of the order parameters used in the previous section. The estimated values of e^2Qq'/h and η' are 185 kHz and 0.05, respectively.¹⁰ Contrary to the quadrupolar coupling, the proton–deuteron dipolar coupling is not affected by the internal rotation of the aniline ring, because the HD-vector ($r = 2.479 \text{ \AA}$)¹¹ is parallel with z -axis. Consequently, the observed dipolar coupling is only averaged by the reorientational motions:

$$D = -\frac{\mu_0 \hbar \gamma_H \gamma_D}{8\pi^2 r^3} S_{zz}, \quad (18)$$

where μ_0 is permeability of vacuum, $\hbar = h/2\pi$, and γ_H and γ_D are gyromagnetic ratios of the proton and deuteron, respectively.

Only the absolute values of the quadrupolar and dipolar couplings can be obtained from the spectrum. Consequently, only the absolute values of the orientational order parameters S_{zz} and $S_{xx} - S_{yy}$ can be solved from Eqs. (17) and (18). However, it is known that the long axis of d_2 -EBBA molecule tends to orient parallel with the external magnetic field, and hence positive value for S_{zz} is expected, indicating negative D . The unresolved sign of B still leads to two possible solutions for $S_{xx} - S_{yy}$, which are shown in Fig. 4.

The above orientational order parameters are not necessarily expressed in the principal axis system (PAS) of the orientation tensor of d_2 -EBBA. Quite often it is assumed that one single orientational order parameter is sufficient to describe the reorientational motions of liquid crystal molecules in a nematic phase. In that case $S_{xx} - S_{yy} = (3/2)\sin^2 \theta \cos 2\phi S$ and $S_{zz} = (1/2)(3\cos^2 \theta - 1)S$, where θ is the angle between the symmetry (long) axis of the mol-

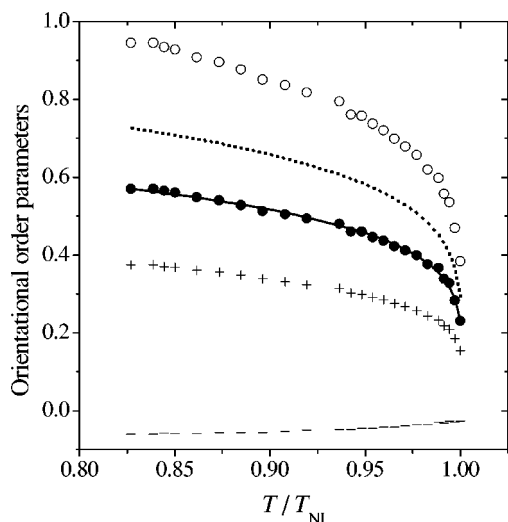


FIG. 4. The orientational order parameters of EBBA calculated from the dipolar and quadrupolar couplings obtained from the ^2H NMR spectrum: S_{zz} (●), and $S_{xx} - S_{yy}$ for positive (+) and negative (−) values of the quadrupolar coupling, respectively. Orientational order parameter of the symmetry axis of EBBA, S (○), calculated by assuming cylindrically symmetric reorientational behavior. Solid line represents the fit of function $\frac{1}{2}(3 \cos^2 \theta - 1)(1 - yT/T_{\text{NI}})^z$ to S_{zz} , and the dotted line represents the behavior of $(1 - yT/T_{\text{NI}})^z$, i.e., the behavior of the orientational order parameter of the symmetry axis of EBBA in case of small biaxiality (see text).

ecule and the z -axis, and ϕ is the angle between the aniline ring plane and the symmetry axis. S is the orientational order parameter of the molecular symmetry axis (corresponding to \bar{P}_2 in the spherical tensor representation), having positive value in d_2 -EBBA. The geometry of d_2 -EBBA suggests that the symmetry axis is near the aniline ring plane and the z -axis direction. Clearly with the negative value of $S_{xx} - S_{yy}$ an unrealistic direction for the symmetry axis would result, i.e., $|\phi| > 45^\circ$. With the positive value of $S_{xx} - S_{yy}$, and assuming that the symmetry axis is in the aniline plane (i.e., $\phi \approx 0$), an angle of $\theta = 31^\circ$ with z -axis is obtained. It is somewhat larger than expected, and because the S values are also somewhat too high (see Fig. 4) as compared to existing observed values,¹² we conclude that one orientational order parameter is probably not sufficient to describe the reorientational motions of d_2 -EBBA.

With two measured couplings it is not possible to determine two independent orientational order parameters and the direction of PAS. However, if we assume that two of the PAS axes (axes α and γ) are in the aniline ring plane, the following result is obtained:

$$S_{xx} - S_{yy} = \frac{3}{2}(1 - \cos^2 \theta)S_{\gamma\gamma} + \frac{1}{2}(\cos^2 \theta + 1)(S_{\alpha\alpha} - S_{\beta\beta}) \\ \approx \frac{1}{2}(\cos^2 \theta + 1)(S_{\alpha\alpha} - S_{\beta\beta}), \quad (19)$$

$$S_{zz} = \frac{1}{2}(3 \cos^2 \theta - 1)S_{\gamma\gamma} + \frac{1}{2}(1 - \cos^2 \theta)(S_{\alpha\alpha} - S_{\beta\beta}) \\ \approx \frac{1}{2}(3 \cos^2 \theta - 1)S_{\gamma\gamma}, \quad (20)$$

where the approximation is done for small θ (i.e., for the angle between z - and γ -axis). If it is valid, the largest orientational order parameter $S_{\gamma\gamma}$ ($= \bar{P}_2$), describing the reorien-

tational motions of the long molecular principal axis, is directly proportional to S_{zz} . The angle θ can be estimated by applying suitable model function for the temperature (T) dependence of $S_{\gamma\gamma}$. Such a function is, for example, the so-called Haller function $S_{\gamma\gamma}(T) = (1 - yT/T_{\text{NI}})^z$, where T_{NI} is the nematic to isotropic transition temperature, and y and z are adjustable parameters.¹³ Fitting of the above equation to the measured S_{zz} values gives the parameters $y = 0.9988 \pm 0.0002$, $z = 0.182 \pm 0.004$, and $\theta = 22.3 \pm 0.4^\circ$, where 347 K was chosen as the transition temperature. The fitted values are comparable to the values in other nematic liquid crystals.

B. Temperature dependence of ^{129}Xe shielding

The chemical shift of ^{129}Xe in d_2 -EBBA referenced to the corresponding pure gas signal at 300 K has been measured as a function of temperature. Because the ^{129}Xe shielding of pure xenon gas at small pressure is approximately equal to the unperturbed shielding constant of xenon atom,¹⁴ the shielding induced by the liquid crystal medium is obtained directly from the measured chemical shift. The ^{129}Xe in d_2 -EBBA is found to be deshielded, as shown in Fig. 5 as a function of reduced temperature (T/T_{NI}). In order to observe the purely microscopic part of the medium shielding, the bulk susceptibility correction is applied, which is for long cylindrical sample parallel with external magnetic field¹⁵

$$\sigma_b = -\frac{1}{3} \left[\chi + \frac{2}{3} \Delta\chi \bar{P}_2 \right] \frac{\rho}{M}. \quad (21)$$

Here χ ($-1.5 \times 10^{-9} \text{ m}^3/\text{mol}$) and $\Delta\chi$ ($0.6 \times 10^{-9} \text{ m}^3/\text{mol}$) are the isotropic part and the anisotropy of the molecular susceptibility tensor, respectively, where typical values for molecules with two benzene rings are used.¹⁶ The orientational order parameter $\bar{P}_2 = [(1 - yT/T_{\text{NI}})^z]$ was determined above, and the molar mass M is 281.4 g/mol for d_2 -EBBA. Number density ρ of EBBA was derived from the measurements of Bahadur *et al.* as discussed below. The bulk susceptibility corrected microscopic medium shielding is shown in Fig. 5.

According to the pairwise additivity model of Eq. (14), the density dependence of the noble gas shielding can be removed by dividing the experimental values with the density of the liquid crystal. The density of pure EBBA was measured as a function of temperature by Bahadur *et al.*¹⁷ They found it to change linearly in isotropic and nematic phases, having slightly different isobaric thermal expansion coefficients [$\alpha = -(1/\rho)(\partial\rho/\partial T)_P$]; $8.09 \times 10^{-4} \text{ K}^{-1}$ and $9.92 \times 10^{-4} \text{ K}^{-1}$, respectively. Furthermore, a small density jump is observed in the nematic–isotropic phase transition. The phase transition temperature is five degrees lower in our sample (347 K) as compared to the value obtained from the density measurements. That is due to the presence of xenon gas in the sample (small overpressure). However, we assume that the phase transition temperature has only shifted, and the values obtained by Bahadur *et al.* are still applicable in our case. The ^{129}Xe shielding divided by the density of EBBA is shown in Fig. 6. Then, the residual temperature dependence of ^{129}Xe shielding in isotropic phase can be modelled with

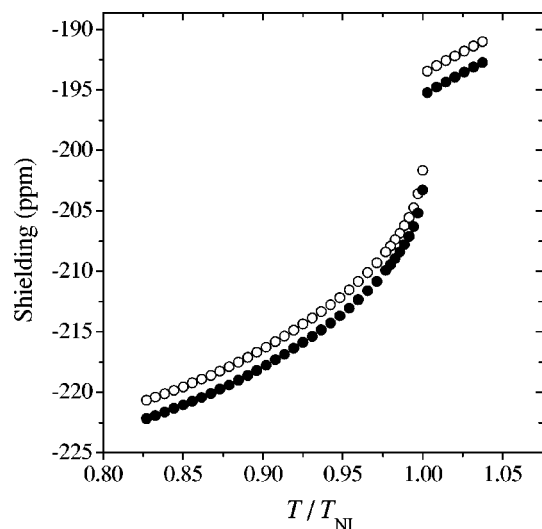


FIG. 5. Medium induced shielding σ_m of ^{129}Xe in EBBA (○) and the bulk susceptibility corrected value $\sigma_m - \sigma_b$ (●).

σ_0 and ϵ (with T_0 fixed to T_{NI}). The resulting fit is shown in Fig. 6 and the parameter values are given in Table I.

In the nematic phase, the anisotropic part of the shielding also enters into the equation due to the nonvanishing orientational order of the liquid crystal. The Haller function with the values obtained in the previous section is used to describe the temperature dependence of $\bar{P}_2(T)$. The values of σ_0 and ϵ in the nematic phase are fixed to the values obtained in the isotropic phase. That assumption is justified by a previous investigation of ^{129}Xe shielding in the so-called critical mixture of EBBA and ZLI1167.¹⁸ It shows that the small difference between the nematic phase value of the isotropic part of ^{129}Xe shielding and the value extrapolated from the isotropic phase can be explained by the effect of the liquid crystal density [see Eq. (14)]. Consequently, the nem-

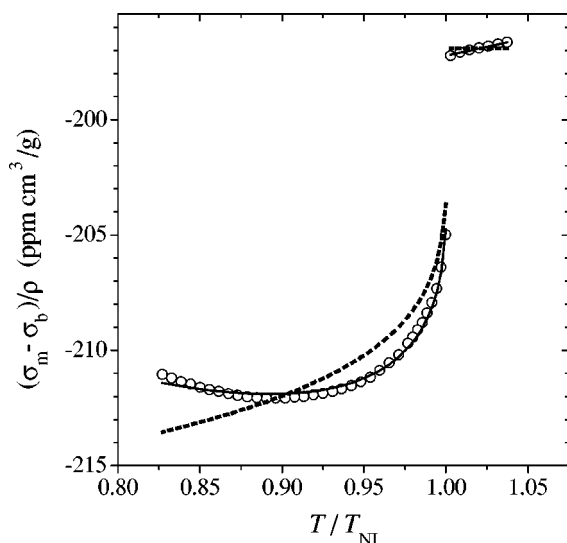


FIG. 6. Bulk susceptibility corrected medium shielding of ^{129}Xe in EBBA divided by the density of EBBA (○). The solid and dashed lines represent least squares fits of Eq. (14), where ϵ and $\Delta\epsilon$ have been refined (fit A in Table I) or fixed to zero (fit B in Table I), respectively.

TABLE I. The refined and constrained values of the parameters of Eq. (14) resulting from least squares fits of ^{129}Xe shielding data in d_2 -EBBA. In fit A, ϵ and $\Delta\epsilon$ were adjustable parameters, whereas in fit B they were fixed to zero.

	Fit A		Fit B	
	Isotropic	Nematic	Isotropic	Nematic
σ_0 (ppm cm ³ g ⁻¹)	-197.2	-197.2 ^a	-196.9	-196.9 ^a
ϵ (10 ⁻⁴ K ⁻¹)	2.3	2.3 ^a	0 ^b	0 ^b
$\Delta\sigma_0$ (ppm cm ³ g ⁻¹)	...	-38.2	...	-34.3
$\Delta\epsilon$ (10 ⁻⁴ K ⁻¹)	...	-63.6	...	0 ^b
y for $\bar{P}_2(T)$...	0.9988 ^c	...	0.9988 ^c
z for $\bar{P}_2(T)$...	0.182 ^c	...	0.182 ^c
T_{NI} (K)	347 ^b	347 ^b	347 ^b	347 ^b

^aFixed to the isotropic phase value.

^bFixed (see the text).

^cDetermined from the ^2H spectra of deuterated EBBA.

atic phase fit for ^{129}Xe shielding requires only two adjustable parameters, $\Delta\sigma_0$ and $\Delta\epsilon$, shown in Table I. The resulting temperature behavior is shown in Fig. 6.

A small change of the fixed values of σ_0 and ϵ would not have changed the quality nor the fitting results of the nematic phase significantly. However, the release of those parameters would have changed ϵ to an extent which would have disagreed with the earlier observation of the isotropic part behavior of the shielding in the nematic phase.¹⁸ Consequently, the fitted results should be reliable, and the remaining deviation between the model and observations may be attributed to the linear approximation used in the derivation of the anisotropic part of the shielding [see Eq. (13)].

The compatibility of the above fit implies that the pairwise additivity approximation of the noble gas shielding is legitimate. The much higher value of α ($8.09 \times 10^{-4} \text{ K}^{-1}$) as compared to ϵ ($2.3 \times 10^{-4} \text{ K}^{-1}$) in the isotropic phase indicates that the change of the solvent density has more effect on the temperature dependence of the ^{129}Xe shielding than the change of the Xe-EBBA molecule pair correlation function. Moreover, both of them decrease the medium effect with increasing temperature and hence with decreasing density. On the contrary, the nematic phase fit of Eq. (14) gives the somewhat surprising result that the value of $\Delta\epsilon$ ($-63.6 \times 10^{-4} \text{ K}^{-1}$) is much larger and opposite to α ($9.92 \times 10^{-4} \text{ K}^{-1}$), indicating that the solute-solvent pair correlation has an important role in the change of the anisotropic part of the shielding. The consequence is that the average anisotropy of the *local* shielding tensor decreases (i.e., the anisotropic contribution without the effect of orientational order parameter) with decreasing temperature. Thus one important new result of the present work is that the anisotropic part of the shielding has a pronounced additional temperature dependence, which is *opposite* to that of the isotropic part.

The importance of the temperature dependence of $\langle\sigma\rangle_{r_1}$ and $\langle\Delta\sigma\rangle_{r_1}$ can be revealed by refitting the ^{129}Xe shieldings with ϵ and $\Delta\epsilon$ fixed to zero, which corresponds to the approximation introduced by Lounila *et al.*⁸ Clearly, the resulting poor fit shown in Fig. 6 proves that the temperature dependence of $\langle\sigma\rangle_{r_1}$ and $\langle\Delta\sigma\rangle_{r_1}$ must be taken into account.

Finally, it should be noted that the developed approach may also be utilized to explain the behavior of the quadrupolar coupling of noble gas isotopes in liquid crystals.

V. CONCLUSIONS

We have demonstrated that the medium induced nuclear magnetic shielding of a noble gas in a liquid crystal solvent is directly related to the liquid crystal orientational order parameters in the form of the linear combination of Eq. (9). Moreover, the reasonable assumption of pairwise additivity of the medium induced shielding is shown to lead to a particularly useful result. The resulting isotropic and anisotropic shielding contributions are directly proportional to the density of the liquid crystal, and the anisotropic part is also proportional to the second rank orientational order parameter of the liquid crystal. The results obtained for ^{129}Xe in the nematic liquid crystal d_2 -EBBA support the pairwise additivity approximation. As a new result, the temperature dependence of the anisotropic part of the shielding is found to be significantly influenced by the noble gas atom–liquid crystal molecule pair correlation function.

ACKNOWLEDGMENTS

The authors are grateful to the Academy of Finland for financial support.

- ¹J. Jokisaari, Prog. Nucl. Magn. Reson. Spectrosc. **26**, 1 (1994).
- ²P. J. Barrie and J. Klinowski, Prog. Nucl. Magn. Reson. Spectrosc. **24**, 91 (1992).
- ³T. G. Walker and W. Happer, Rev. Mod. Phys. **69**, 629 (1997).
- ⁴W. E. Lamb, Jr., Phys. Rev. **70**, 460 (1941).
- ⁵M. Luhmer and K. Bartik, J. Phys. Chem. A **101**, 5278 (1997).
- ⁶C. Zannoni, in *The Molecular Physics of Liquid Crystals*, edited by G. R. Luckhurst and G. W. Gray (Academic, London, 1979).
- ⁷C. G. Gray and K. E. Gubbins, *Theory of Molecular Fluids* (Clarendon Press, Oxford, 1984), Vol. 1.
- ⁸J. Lounila, O. Muenster, J. Jokisaari, and P. Diehl, J. Chem. Phys. **97**, 8977 (1992).
- ⁹R. J. Wittebort, E. T. Olejniczak, and R. F. Griffin, J. Chem. Phys. **86**, 5411 (1987).
- ¹⁰J. W. Emsley and J. C. Lindon, *NMR Spectroscopy Using Liquid Crystal Solvents* (Pergamon, New York, 1975).
- ¹¹M. D. Harmony, V. M. Laurie, R. L. Kuczkowski, R. H. Schwendeman, D. A. Ramsay, F. J. Lowas, W. J. Lafferty, and A. G. Maki, J. Phys. Chem. Ref. Data **8**, 619 (1979).
- ¹²G. R. Luckhurst, in *The Molecular Physics of Liquid Crystals*, edited by G. R. Luckhurst and G. W. Gray (Academic, London, 1979).
- ¹³I. Haller, Prog. Solid State Chem. **10**, 103 (1982).
- ¹⁴A. K. Jameson, C. J. Jameson, and H. S. Gutowsky, J. Chem. Phys. **53**, 2310 (1970).
- ¹⁵A. D. Buckingham and E. D. Burnell, J. Am. Chem. Soc. **89**, 3341 (1967).
- ¹⁶W. H. de Jeu, *Physical Properties of Liquid Crystalline Materials* (Gordon and Breach, New York, 1980).
- ¹⁷B. Bahadur and S. Chandra, J. Phys. C **9**, 5 (1976).
- ¹⁸J. Jokisaari and P. Diehl, Liq. Cryst. **7**, 739 (1990).